**ISSN 1454 - 8003**
**Proceedings of 2022 International Conference on Hydraulics and Pneumatics - HERVEX**
*November 9-10, Băile Govora, Romania*

# PREDICTIVE MONITORING OF HORIZONTAL AXIS WIND TURBINE ROTOR BLADES STRENGTH

Prof. PhD. Dr.Sc. **Viorel BOSTAN[1],** Prof. PhD. Dr.Sc. **Valeriu DULGHERU[1,*],**
Assoc. prof. PhD. **Marin GUȚU[1]**

[1] Technical University of Moldova

* valeriu.dulgheru@bpm.utm.md

***Abstract:*** *Wind turbine blades are subjected to complex environmental and mechanical loads during the operating period. To reduce and optimize maintenance costs, a detailed understanding of the degradation and failure mechanisms of wind turbines is required. This is important for reliable prediction of failure events, planning of maintenance activities and mitigation of degradation processes. The paper presents the main failures of mega wind turbine blades, their analysis methods, performing extensive numerical modeling of a blade and determining areas with stress and deformation concentrations, establishing with higher precision the location of critical areas in order to implement the predictive monitoring system of the wind turbine blades state.*

***Keywords:*** *Wind turbine, blade, numerical modeling, stresses, strains, predictability*

## 1. Introduction

Wind turbine blades are subjected to complex environmental and mechanical loads during their service life, including cyclic deformation, precipitation, erosive particles, freezing, high humidity and temperature variations, but also extraordinary events such as shipping damage, bird strikes and electric discharges [1, 2]. To reduce and optimize maintenance costs, a detailed understanding of the degradation and failure mechanisms of wind turbines is required. This is important for reliable prediction of failure events, planning of maintenance activities and mitigation of degradation processes. For wind turbine blades, life extension is one of the best strategies for using them after 25 years of operation.
However, accidents involving structural failures of wind turbine blades are not uncommon. It is reported [2] that, with approximately 700,000 blades in service globally, there are an average of 3800 blade failure incidents each year.

## 2. Wind turbine blades failure mechanisms

### *2.1 Methods of analyzing the failure mechanisms of wind turbine blades*

Wind turbine blade damage can be classified as surface damage (surface microcracks and coatings), resin and/or interface damage (delamination, resin defects), and structural element damage (fiber breakage or bending) [1,2]. Surface defects can be caused by erosion (caused by rain, sand and hail) or impacts with small objects. The damaged and rough surface reduces the aerodynamic performance of the blade. It does not disrupt the operation of the wind turbine, but surface defects grow and can lead to structural damage of the blade.
In general, the failure mechanisms of wind turbine blades are analyzed using the following main methods:

- post-destruction analysis of damaged blades;
- full-scale testing of blades in laboratories with video observation and structural condition monitoring;
- analysis of databases and collection of incident reports;
- direct monitoring of blade deformation and degradation during operation (e.g. using non-destructive testing and structural condition monitoring methods);

- testing the design of sub-components (e.g. beam), reproducing parts or elements of the blades (e.g. joints or sandwiches);
- computational modeling of blade deformation and damage.

**Direct monitoring of wind turbine blade deformation and damage** can be performed using non-destructive testing methods and structural health monitoring methods [3]. Sensors are attached or embedded in the blades and deformation and damage events are monitored. While structural health monitoring is typically developed for blade control, it can also be used to understand failure mechanisms. Such experiments are undertaken to investigate blade surface erosion. A more detailed analysis is provided in the paper [3].

While **computational modeling of wind turbine blade degradation** is one of the most effective approaches to failure mechanism analysis, the models typically include some predefined and assumed damage mechanisms. For example, a static analysis is done to establish the critical area of the blade and then fatigue crack propagation in that area is simulated.

Computational models are quite efficient and have a wide range of applications. However, their application requires a prior knowledge of the expected damage mechanisms.

### *2.2 The critical areas of the wind turbine blade*

Several segments of wind turbine blades are particularly susceptible to degradation. Among them, the segments subjected to the most intense loads (tip and leading edge), transition sectors (for example, the transition zone from the cylinder to the aerodynamic surface and the transition of the composite layer to a lower thickness), interface portions (with adhesive layers, e.g. trailing edge). According to research [4] the most affected areas of the blade are: near the root (30–35% of the chord length from the root) and near the tip (70% in the chord length from the root of the blade), the root of the blade, the trailing edge on the high pressure side and leading edge.

The main damage mechanisms in critical areas:

*Blade tip.* Because the tip velocity is the highest, the erosion and resulting damage to the leading and trailing edges is much more intense near the tip. Moreover, lightning can strike the blades near the tip and cause the skin to separate near the tip or from the spar [5].

*Leading edge.* As a rule, it is subjected to raindrops, hail, sand and frequent impacts. If surface erosion is not repaired quickly, it can lead to laminates cracking or allow water to enter the bonding area [5].

*Trailing edge.* The trailing edge of wind turbine blades can fail by peeling of the adhesive joint (e.g. due to peel stresses) and/or by buckling of the sandwich panels. Buckling can lead to final failure of the adhesive joint on the running board at much lower than maximum loads.

*Areas of thickness transitions, hub portion:* Other potentially damaging sectors are in the transition zone from circular section to airfoil, due to the sudden transition from thick laminate to fine geometry and large laminated panels in the area of the maximum chord section that can be susceptible to buckling [5].

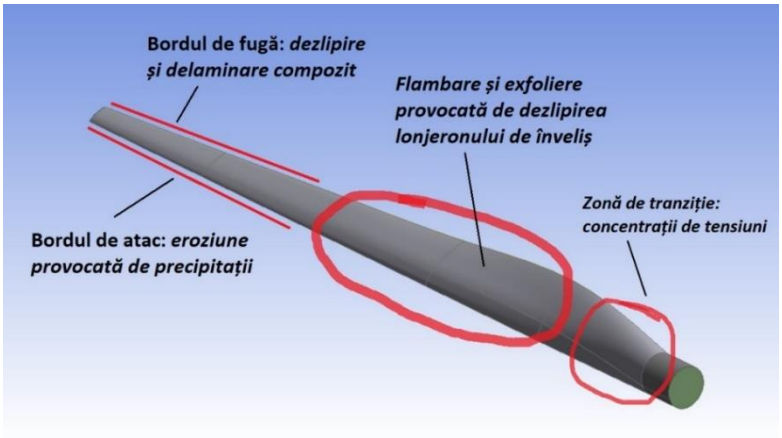


**Fig. 1.** The locations of the damage mechanisms of a wind turbine blade

*Adhesive joints/Bond Lines:* The leading and trailing edge joints between the skin and the internal stiffeners can deteriorate or peel off, leading to buckling of the structures [5]. Blade destruction can occur if the spar detaches from the skin and buckles. According to [4], the blade failure mechanism most often observed are transverse cracks in the area of the maximum chord section (initiated as a detachment of the outer layer from the sandwich core) and detachment of the stiffening ribs from the blade shell in

the transition zone from base (triggered by peel stresses on the adhesive bonding portions). These effects are amplified by manufacturing defects and blade torsional stresses [4]. Figure 1 shows a sketch of the locations of commonly observed damage mechanisms of a wind turbine blade.
Thus, the most endangered sectors of the blades of a wind turbine are the protruding parts (tip, trailing edge), areas with transition sections and those where structural elements are bonded. Fortifying these areas can significantly increase the durability and service life of wind turbine blades.
Figure 2 shows some images of damaged wind turbines with the power of over 1 MW. As can be seen, the location of blade damage is in the buckling zone, at a distance between 0.3 and 0.5 of the rotor radius. According to the research results presented by the authors [2] blade failures occur most of the time in operating conditions that fall within nominal parameters such as wind speed and operating period. Such destructions are consequences of non-compliance with manufacturing technology. Good interaction between material selection, structural design and manufacturing process is required to improve the structural integrity of blades.

**Fig. 2.** Location and appearance of damage on operating wind turbine blades

A finite element calculation model of the strength of a typical blade is presented below. The purpose of this numerical simulation of blade stress conditions is to establish the critical areas and determine the equivalent stresses and strains.

## 3. Numerical modeling of a blade and determination of stress and strain concentration areas

The rotor geometry designed in SolidWorks software was then imported into the DesignModeler program in the ANSYS Workbench environment where the fluid domain was created. To simplify CFD (Computational fluid dynamics) analysis and to save calculation time, 1/3 of the entire domain was modeled.

**Table 1:** Constructive-functional parameters of the analyzed rotor

| | |
|---|---|
| Nominal power, MW | 1.5 - 3 |
| Nominal rotor speed, min-1 | 18 - 20 |
| Wind speed, m/s | 10 - 20 |
| Rotor diameter, m | 83 |
| Variation of shell and spar thickness, m | 0.1 – 0.005 |

A CFD volume including 120° of the rotor was created with a single blade assuming periodic conditions. At the same time, the tower and the ground were neglected. The dimensions of the computational fluid domain were chosen taking into account the best practices and recommendations presented in research [6, 7] to ensure free flow without influencing the domain boundaries. A typical wind turbine rotor with the following input parameters was considered for the simulations (table 1).
To simplify the structural analysis it has been assumed that the composite material can be homogenized by the following orthotropic material properties, Table 2. These values are representative of the properties of composite materials used in real wind turbine blades.

**Table 2:** Properties of the used material

| | |
|---|---|
| Density (kg/m^3) | *1550* |
| Young-X Modulus (Pa) | *1.1375E+11* |
| Young-Y Modulus (Pa) | *7.583E+09* |
| Young-Z Modulus (Pa) | *7.583E+09* |
| Poisson's ratio-XY | *0.32* |
| Poisson's ratio-YZ | *0.37* |
| Poisson's ratio-XZ | *0.35* |
| Shear Modulus-XY(Pa) | *5.446E+09* |
| Shear Modulus-YZ (Pa) | *2.964E+09* |
| Shear Modulus-XZ (Pa) | *2.964E+09* |

Among all the simulation steps, the finite element mesh generation step is the most important. The accuracy of the numerical calculation is determined, first of all, by the quality of the mesh, the density and distribution of nodes in key areas of the computational domain. Such area is near the blade surface where the boundary layer forms. In these areas the elements have been properly refined to correctly capture the strong variations in the flow parameters. Also, transitions from fine mesh to coarse mesh areas have been handled carefully, as too abrupt a transition can alter the accuracy of the calculation. The fluid domain was divided into ~3000 000 elements.

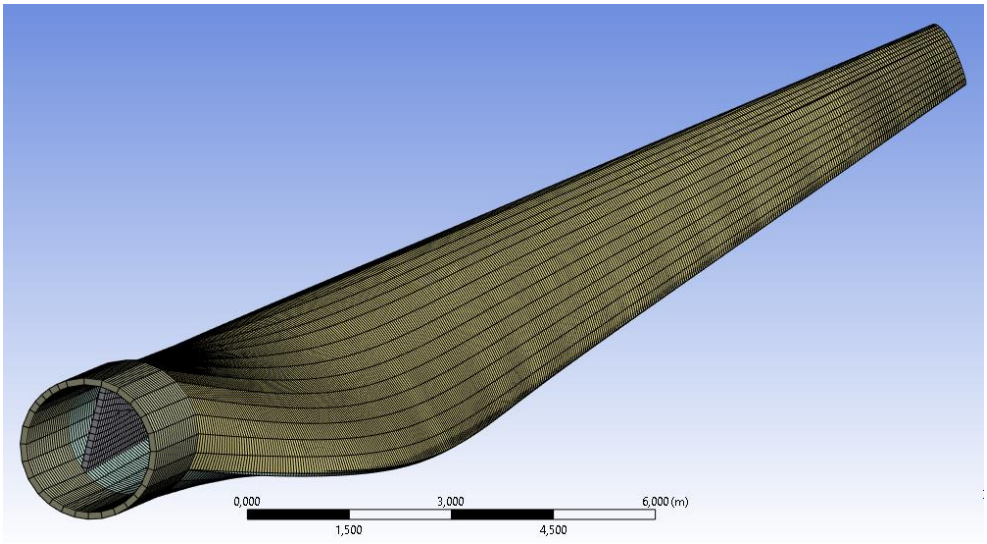


**Fig. 3.** Wind turbine blade mesh details

This value was accepted according to the mesh refinement study presented in the research [8]. Details of the blade shell discretization are shown in figure 3. The rotor was simulated under different boundary conditions, such as wind speed of 10 - 20 m/s and rotation speed corresponding to the nominal one 18 - 20 $min^{-1}$. To check the correctness of the settings, Fig. 4 illustrates the velocity vectors distributed over the blade surface at the nominal speed of 18 $min^{-1}$ (wind speed of 10 m/s).
The air pressure variation diagram passing through the rotor was also drawn, Fig. 5. This corresponds to the physical model according to indications of the researchers [8].

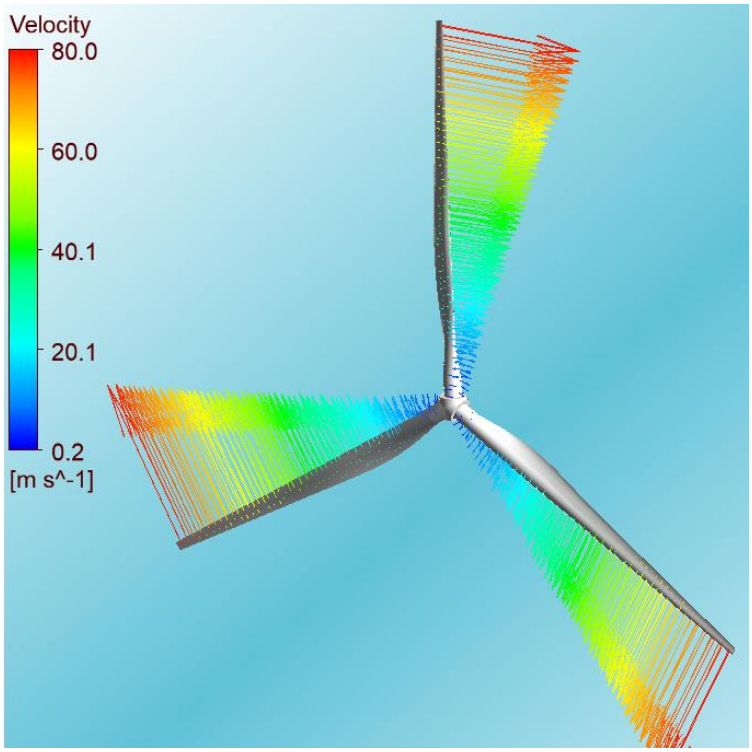


**Fig. 4.** Wind turbine rotor model simulated at 10 m/s wind speed

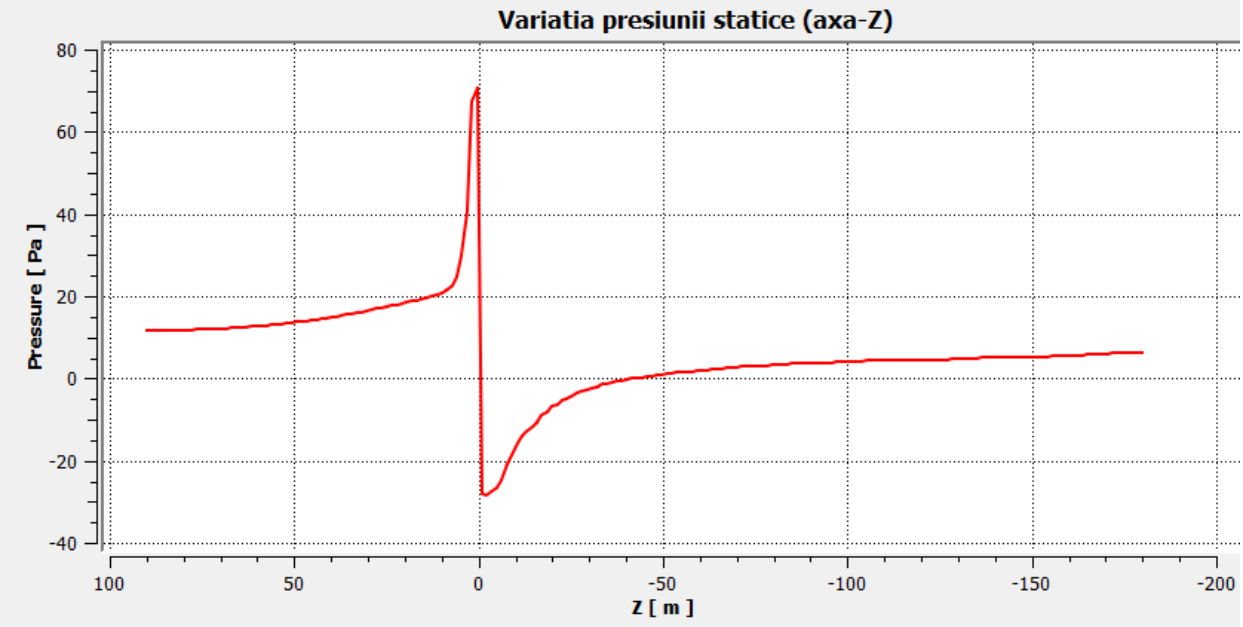


**Fig. 5.** Variation of air pressure in the turbine rotor section

Figure 6 shows the pressure distribution on the blade surface at the wind speed of 10 m/s. Such pressure distribution obtained as a result of aerodynamic effects for the whole range of wind speeds was considered as the main task in the calculation model. Thus, the blade is subjected to complex bending-torsional stresses. Compared to the real loads that include the gravity, in the simulations it was neglected.

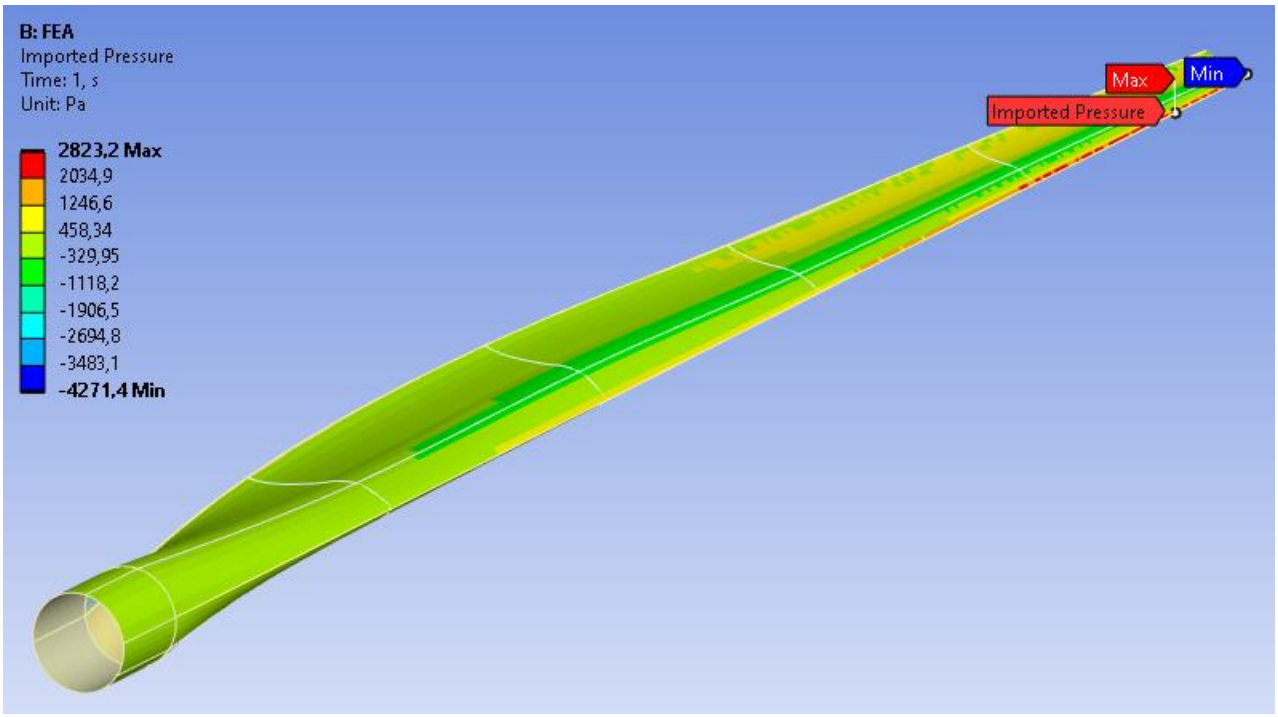


**Fig. 6.** Fluid pressure distribution on the blade surface

After performing the blade simulations, the results of interest were extracted. The distribution of the equivalent stresses (von-Misses) and the location of the concentrations are shown in figure 7. These are the maximum values (≈ 48 MPa) corresponding to the wind speed of 16 m/s. For the nominal wind speed (≈ 11 m/s) the value of the equivalent stresses is ≈ 35 MPa. For comparison, the tensile strength of the epoxy resin adhesive used in the blades structures is 30 – 40 MPa. It is obvious that the operation of the wind turbine at slightly higher than nominal wind speeds must be limited.

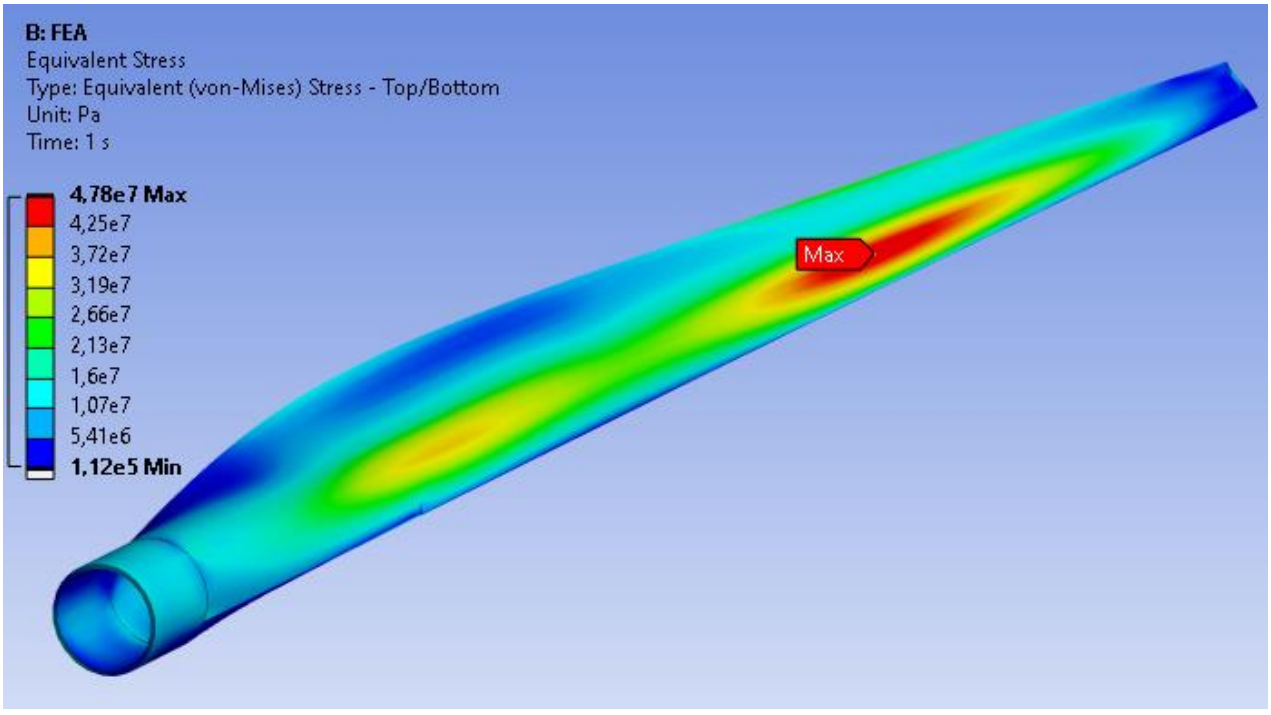


**Fig. 7.** Equivalent (Von-Mises) stresses distribution on the blade shell

Figure 8 shows the equivalent elastic strain in the blade shell and certain locations where concentrations occur. An illustrative case is presented for wind speed V =12 m/s. For the other wind speeds the locations of the critical areas are the same.

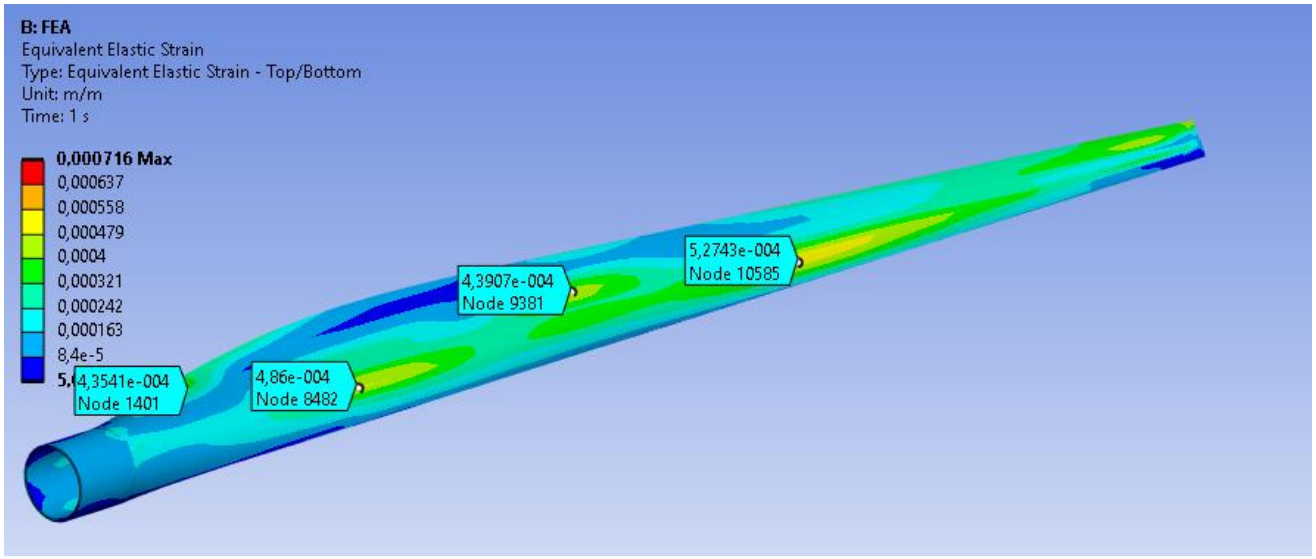


**Fig. 8.** Equivalent elastic strain distribution (a case for V =12 m/s)

Below is a diagram containing all the values of the equivalent elastic strain depending on the wind speed, figure 9. The distribution of the equivalent elastic strain in the blade shell is presented for the minimum and maximum values that coincide with the locations along the longitudinal axis (radius rotor – 0.17r and 0.68r). The diagram also shows the wind turbine rotor power values obtained from the relationship: $P = \omega \cdot T$, where $\omega = 2$ rad/s is kept constant at wind speeds greater than 12 m/s, and T – the torque developed by the turbine rotor depending on the wind speed.

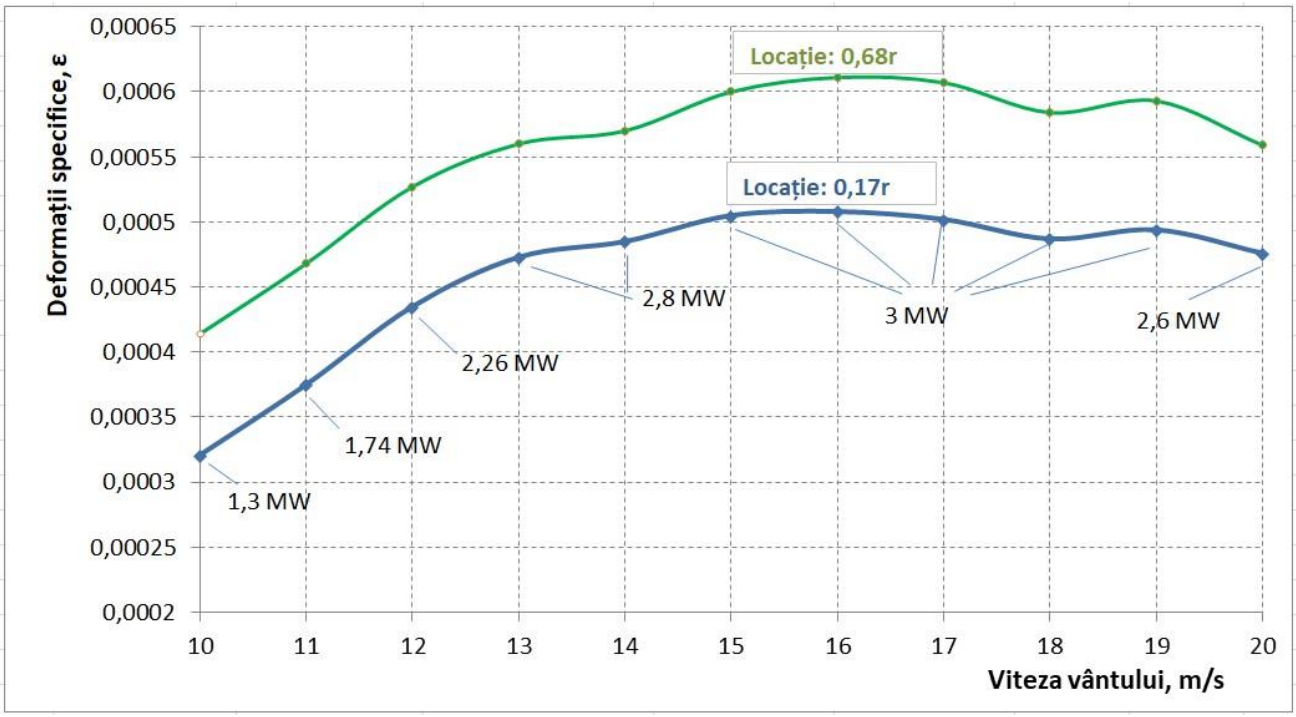


**Fig. 9.** Results diagram of wind turbine blade simulation

Determination of the critical areas with higher precision for a particular blade model requires the direct simulation of it. However, with the help of the information in Figures 1, 2 and 8, priority locations can be established in order to implement the wind turbine blade condition predictive monitoring system.

**References**

[1] Mishnaevsky, L., Jr. "Root Causes and Mechanisms of Failure of Wind Turbine Blades: Overview." *Materials (Basel)* 15, no. 9 (April 2022): 2959. https://doi.org/10.3390/ma15092959.

[2] Chen, X. "Fracture of wind turbine blades in operation - Part I: A comprehensive forensic investigation." *Wind Energy* 21, no. 11 (November 2018): 1046– 1063. https://doi.org/10.1002/we.2212.

[3] McGugan, M., and L. Mishnaevsky, Jr. "Damage Mechanism Based Approach to the Structural Health Monitoring of Wind Turbine Blades." *Coatings* 10, no. 12 (2020): 1223. https://doi.org/10.3390/coatings10121223.

[4] Jensen, Find, et al. *Cost and Risk Tool for Interim and Preventive Repair (CORTIR)*. Bladena Report. EUDP Project 64018-0507 – Final Report, 2021.

[5] Robinson, C. M. E., E. S. Paramasivam, E. A. Taylor, A. J. T. Morrison, and E. D. Sanderson. *Study and Development of a Methodology for the Estimation of the Risk and Harm to Persons from Wind Turbines.* London, Health and Safety Executive, 2013.

[6] Wang, Z., G. C. Tsai, and Y. B. Chen. "One-Way Fluid-Structure Interaction Simulation of an Offshore Wind Turbine." *International Journal of Engineering and Technology Innovation* 4, no. 3 (2014): 127-137.

[7] Kelele, Hailay Kiros, Torbjørn Kirstian Nielsen, Lars Froyd, and Mulu Bayray Kahsay. "Catchment Based Aerodynamic Performance Analysis of Small Wind Turbine Using a Single Blade Concept for a Low Cost of Energy." *Energies* 13, no. 21 (2020): 5838. https://doi.org/10.3390/en13215838.

[8] Lachance-Barrett, S., and E. Corona. "Wind Turbine Blade FSI (Part 1) - Numerical Solution." September 27, 2019. Accessed October 12, 2022. *Fluent Learning Modules*. https://confluence.cornell.edu/.